Detection of rocket exhaust plumes in the upper troposphere, stratosphere and mesosphere - Impact on atmospheric composition

Christiane Voigt,**, Ulrich Schumann* and Kaspar Graf**

** Deutsches Zentrum für Luft- und Raumfahrt (DLR)*
Institut für Physik der Atmosphäre
Oberpfaffenhofen
D-82234 Wessling
Germany

*** Johannes-Gutenberg-Universität Mainz*
Institut für Physik der Atmosphäre
Johannes-Joachim-Becher-Weg 21
D-55099 Mainz
Germany

Abstract

Rockets are the only direct anthropogenic emission sources into the upper atmosphere. Depending on the type of propellant significant amounts of aluminum oxide (Al_2O_3) particles and trace gases such as chlorine species, CO, N_2, H_2, H_2O, and CO_2 are injected into the atmosphere. These emissions strongly perturb local aerosol and trace gas levels, can lead to global ozone loss in the stratosphere and to enhanced cloud formation in the mesosphere.
Here we summarize aircraft measurements in the exhaust plumes from several large space shuttles as well as smaller rockets and investigate local changes of the lower stratospheric composition. While the resulting impact of rocket emissions on global stratospheric ozone levels may be small, large uncertainties remain concerning individual ozone loss reactions and regional ozone changes. The stratospheric perturbations of trace species by rocket plumes are compared to natural and anthropogenic sources such as volcanism, meteoritic input and aviation.
In addition, we present a unique observation of ice particle formation in the exhaust plume from an Ariane5 launch vehicle. The evolution of the rocket contrail near 14 km altitude in the tropopause region could be followed for almost two hours before local sunset in Meteosat-9 images. Enhanced ice particle formation related to rocket emissions had been reported previously in the mesosphere. In altitudes near and above 85 km rocket exhaust plumes regionally increase the water vapor concentrations and lead to the formation of mesospheric clouds in polar and extra-polar regions.

1. Introduction

Rocket plumes currently represent a tiny fraction of the total anthropogenic emissions to the atmosphere, still prudence is required to carefully assess their envidonmental impact. Space traffic is expected to increase in coming decades [1], hence the local and global perturbations of the atmospheric composition by rocket exhaust have to be evaluated and the atmospheric processes occurring in the plumes at all scales have to be understood. While atmospheric composition changes related to rocket emissions near the launch site have an impact on air quality and

maybe of transient nature in the troposphere, long-term effects are expected in the stratosphere, currently leading to global total ozone loss in the range of ~0.03% [2].
The atmospheric effects of rocket emissions depend of the propellant type. Solid rocket motors (SRMs) consisting of aluminium fuel and an ammonium perchlorate (NH_4ClO_4) oxidizer represent only a fraction of the total rocket emission inventory. SRM are often combined with cryogenic rocked engines with liquid oxygen and liquid hydrogen (LOX/H_2) compartments to increase thrust. This engine type powers for example the expendable rocket launch system Ariane5. In addition, a liquid oxygen/kerosene (LOX/kerosene) booster rocket system is commonly used in space industry e.g. for the for the Soyuz launch vehicle.
Here we summarize previous observations of rocket exhaust plumes from several rocket types performed on aircraft in the lowest stratosphere. The impact of rocket emissions on stratospheric ozone levels is discussed and the rocket emissions are compared to other emission inventories. In addition, we present new observational evidence of rocket contrail formation near 14 km from Seviri (Spinning Enhanced Visible and Infrared Imager) images on the Meteosat-9 satellite and compare our observations to enhanced mesospheric cloud formation at higher altitudes above 80 km.

2. Aircraft measurements of stratospheric perturbations by rocket exhaust plumes

While direct measurements of rocket emissions from European launch vehicles are still missing, the exhaust plumes from a space shuttle, a Titan IV, an Athena II, an Atlas II and a Delta II rocket have been probed previously with in-situ instruments on the NASA WB57 high altitude research aircraft. Here we compile and summarize those measurements of rocket exhaust plumes.
The aerosol size distributions of rocket exhaust plumes from two large SRM space shuttles and a Titan IV rocket have been detected in 1996 and 1997 at altitudes between 17.5 and 19 km with a real time particle counter and a grab tank sampling system onboard the WB57 aircraft [3]. Particle number concentrations of several hundred per cm^3 of Al_2O_3 particles in the size range of 0.01 to 4 µm have been observed in 5-min old stratospheric exhaust plumes. The rocket exhaust plumes have a trimodal particle size distribution with modes near 0.005 µm, 0.1 µm, and 2 µm. While the long-lived and hence atmospherically relevant smallest mode contains less than 0.1% of the aluminum mass, more than 99% of the particle mass is concentrated in the largest mode. Similar aerosol concentrations of few hundred per cm^3 have been measured in the stratospheric exhaust plume of a Delta II rocket powered by a combination of solid (NH_4ClO_4/Al) and liquid (LOX/kerosene) propulsion system [4]. The plume has been intercepted six times at plume ages of 12 min to one hour. Extraordinary high amounts of reactive chlorine (up to 45 ppbv ClO) decrease with plume age while ozone loss increases and complete ozone destruction occurs in the 39-min old rocked exhaust plume. The observed local ozone holes are probably promoted by gas phase reactions of the catalytic ClO dimer cycle unique to warm (215K) SRM exhaust plumes.
In addition, the stratospheric exhaust plume of a small Athena II SRM has extensively been probed at plume ages of 4 to 26 minutes after launch near 18 km altitude [5]. The plume has alumina particle abundances near 10000 per cm^3 in the size range between 0.004 and 1.2 µm. 37% of the total surface area (8% of the total mass) is contained in the submicron particle size range with diameters smaller than 1 µm, significantly more than observed in previous studies [3]. Due to its long atmospheric lifetime, this particle size range most influences the stratospheric impact of alumina particles on ozone, and the global ozone loss of heterogeneous reactions on SRM alumina particles may increase the ozone loss due to gas phase chlorine chemistry alone by a factor of 1.5.
The Athena II SRM plume has also been sampled with a single particle aerosol mass spectrometer [6] onboard the WB57. More than 2300 exhaust particles from the Athena II SRM plume and a space shuttle plume have been analyzed. The rocket plume aerosol contains primary and trace components of the aluminum fuel and the combustion catalyst. In addition, chlorine from the oxidizer, iron and elemental carbon are present in the Anthena II rocket plume and nitrate, phosphate and water in the space shuttle plume particles suggesting that the particle composition in the exhaust plumes is very diverse. While most models assume the main abundance of rocket emission products in the gas phase, the extensive detection of components of the rocket fuel, oxidizer, binding agents, and the combustion catalyst in particles leaves open question on the reactivity and on heterogeneous chlorine chemistry on coated alumina particles.
Measurements of reactive nitrogen (NOy) and a nitric acid (HNO_3) in the Athena II SRM plume [7] show NOy mixing ratios above 100 ppbv (parts ber billion by volume) in the less than an half an hour old plume. High nitric acid mixing ratios of more than 50 ppbv infdicate that HNO_3 is a significant plume component, most probably formed by the heterogeneous reaction between $ClONO_2$ and HCl on the emitted alumina particles.
Such high nitric acid concentrations combined with low temperatures (below 215 K) may favor the formation of nitric acid trihydrate (NAT) particles in rocket exhaust plumes [8]. NAT nucleation on ice has frequently been observed in polar stratospheric clouds [9]. A similar process may occur in stratospheric

rocket wakes, as inferred from measurements in 3 exhaust plumes from an Atlas II, a Delta II, and an Athena II rocket.

3. Simulations of regional and global stratospheric ozone loss related to rocket emissions

Local ozone loss and ozone mini holes have been observed in young rocket exhaust plumes during daytime [4]. Here, we summarize simulations of the impact of rocket emissions on regional and global and regional ozone levels. Two- and three-dimensional atmospheric chemistry transport models (CTMs) were used to follow the buildup of exhaust products and their perturbation to stratospheric ozone levels. The CTMs calculate chlorine enhancements < 0.6% above the background due to rocket emissions in 1990 of 9 space shuttles and 3 Titan rockets [10]. Gas phase processes including ozone loss by the ClO dimer catalytic cycle lead to maximum ozone loss of 0.12% in the northern mid-latitude upper stratosphere near 40 km altitude stratosphere.
In addition to gas phase chemistry alone, additional heterogeneous ozone loss on the stratospheric sulfate aerosol layer (SSA) and on polar stratospheric clouds has been calculated with a two-dimensional photochemistry and transport model for the same launch scenario [11]. The model calculates annually averaged global total ozone decreases of 0.006% related to gas phase chemistry only, and of 0.014% including gas phase and heterogeneous reactions on SSA and PSCs. The same model is used to also calculate heterogeneous chlorine activation reaction directly on alumina (aluminum oxide particles) emitted by solid rocket motors using historical launch rates of space shuttles, Titan III, and Titan IV rockets [12]. The time dependent steady state model computes an average global total ozone decrease of 0.025% by the year 1997. About one third of this change results from heterogeneous reactions on alumina emitted by SRMs.
Ozone loss caused by NO and H_2O emissions from hydrazine-fuelled rockets has been calculated with plume and global atmosphere models [13]. Hydrazine fuelled rockets such as the Proton account for about one third of all stratospheric rocket emissions comparable in mass to solid-fuelled rocket emissions. While maximum local and time dependent ozone loss is 21% at 44 km altitude due to the catalytic NO cycle, steady state global ozone loss from 10 Proton launches annually is $1.2*10^{-4}$% hence significantly less effective than ozone destruction by solid-fuelled rockets.
The impact of a future fleet of 1000 hydrocarbon fuelled rockets used potentially for commercial purposes has been investigated recently [14]. These potential emissions would create a persistent layer of black carbon particles in the northern stratosphere leading to changes in the global atmospheric circulation and ozone and temperature distributions.

3. Comparison of the rocket emission inventory to other anthropogenic and natural sources

After having discussed strong local stratospheric perturbations by rocket emissions as detected from aircraft and their impact on the global ozone budget as simulated with a suite of models, we now compare rocket emissions to stratospheric inputs from other sources such as aviation, volcanoes and meteoritic input. The propulsion systems of the present day rocket fleet if at all do not contain significant amounts of sulphur, hence the contribution of rocket emissions to the stratospheric sulphate aerosol layer is negligible. This is as confirmed by lidar observations of the evolution of the stratospheric aerosol layer [15], where no impact of rocket launches can be identified.
Meteorites provide another source of particles into the stratosphere. Most (60%) of the meteoritic mass influx in the atmosphere of 8–30 Gg per year ablates at altitudes above 80 km due to frictional heating. The ablation products recondense, coagulate in the mesosphere and form nanometer-sized smoke particles. The meteoritic smoke particles are then transported with the atmospheric circulation and sediment down, and most of them likely enter the stratosphere over the winter pole. There the meteoritic particles remain more than a year, they become well-mixed and are partly incorporated into the stratospheric sulfate aerosol [16 and references therein].
Averaged over the years 2000 to 2002 the total rocket propellant emission from a fleet of space shuttle, Titan IV, Proton, Long March, Ariane5, Soyuz, Zenit and smaller rocket launch vehicles has been calculated to amount to ~30 Gg per year of which about 9 Gg per year are emitted into the stratosphere [13]. While the total amount rocket emissions into the stratosphere is of similar magnitude as the meteoric influx, the particulate alumina fraction of the rocket emissions in stratosphere is about one third of the total emissions and amounts to ~3 Gg annually.

An assumed ESA rocket fleet of 6 Ariane5 launch vehicles, using SRM and cryogenic LOX/H_2 propellants, two Vega rockets with SRM and two Soyuz with a LOx/kerosene propellant would release about 5 Gg CO_2 into the atmosphere. Even taking into account the emissions from the global rocket fleet, the rocket CO_2 emissions are by 4 to 5 orders of magnitude lower than CO_2 emissions from aviation, which lie in the range of 600000 to 700000 Gg annually.
Similar order of magnitude estimates can be performed for water vapor emissions. We estimate the upper atmospheric water vapor mass (above 100hPa) assuming a water vapor mixing ratio of 3 µmol/mol (ppmv) to >200000 Gg. The assumed ESA rocket fleet emits about 2 Gg H_2O per year, which is about 4 orders of magnitude lower than water formation by methane in the stratosphere of 45000 Gg annually. Another example, water vapor emissions by aviation contribute about 250000 Gg per year to the global water cycle in the troposphere and stratosphere.
Hence while the stratospheric water budget is not significantly perturbed by water emissions from rockets, significant enhancements of mesospheric water levels have been detected regionally and collocated with enhanced mesospheric cloud formation. These observations will be discussed later. Before, we show the first direct observation of water from rocket emissions in the upper troposphere/lower stratosphere region detected from satellite.

4. Contrail formation in an Ariane5 rocket exhaust plume

While formation of ice particles related to rocket exhaust plumes has been reported previously in the mesosphere, we now present first evidence for the formation of ice crystals in the tropopause region and upper troposphere near 14 km altitude. Below this altitude, formation of condensation trails (contrails) is known to be induced by aircraft. Aircraft contrails generally form at cruise altitudes between 8 and 12 km and at temperatures below -42°C [17]. The hot aircraft exhaust mixes with ambient cold and humid air and cools down. When saturation with respect to water is reached, water condenses on liquid and solid plume particles. Then ice can nucleate in the activated aerosol if temperatures are below the ice frost point [17]. When the ambient air is supersaturated with respect to ice, contrails can live for several hours and become persistent.
Young contrails with ages of a few hours are detecable in satellite images of brightness temperatures because of their linear shape, while aged contrails loose their structure and cannot be distinguished from natural cirrus cloudiness.

Here we present the unique case of contrail formation in the exhaust plume from an Ariane5 rocket. The Ariane5 has been launched on 26 November 2010 at 18:39 UTC at the Space Center near Kourou in French Guyana.
The satellite analysis of this launch has been performed with the SEVIRI (Spinning Enhanced Visible and Infrared Imager) instrument on board Meteosat-9 satellite positioned in geostationary orbit at 0°. The SEVIRI images provide information on solar and terrestrial radiation in 12 spectral channels. 11 of the spectral channels have a resolution of 3 km at the sub-satellite point while the High Resolution Visible (HRV) channel 12 provides data with a resolution of 1 km. In addition, the SEVIRI instrument has a high temporal resolution of 15 minutes, which is necessary for the launch analysis and to investigate the cloud life cycle.
As clouds and rocket plumes are small scale and fast moving objects, we employ the high temporal and spatial resolution provided by the HRV channel. As the HRV channel is located in the visual spectrum, no information is available during night time.
Figure 1 shows 6 HRV images for time steps between 18:30 and 20:30 UTC on 26 November 2010. At 18:30 UTC, 9 minutes before the rocket launch, mainly natural cloudiness is detected by the satellite instrument. In 850 hPa near the ground the wind direction is to the west (yellow arrows) and in 100 hPa the wind direction is to the south (green arrows). The Ariane5 flight track from the surface to 20 km altitude is indicated as pink line in each image. After the Ariane5 launch at 18:39 UTC, two effects of rocket emissions can be observed in the satellite images. At 18:45 UTC a line-shaped cloud can be identified and related to the rocket emissions. The line-shaped structure marked by the yellow circles drifts in south-eastern direction within the next 2 hours. In addition there is an exhaust plume marked with the blue arrow drifting westwards.

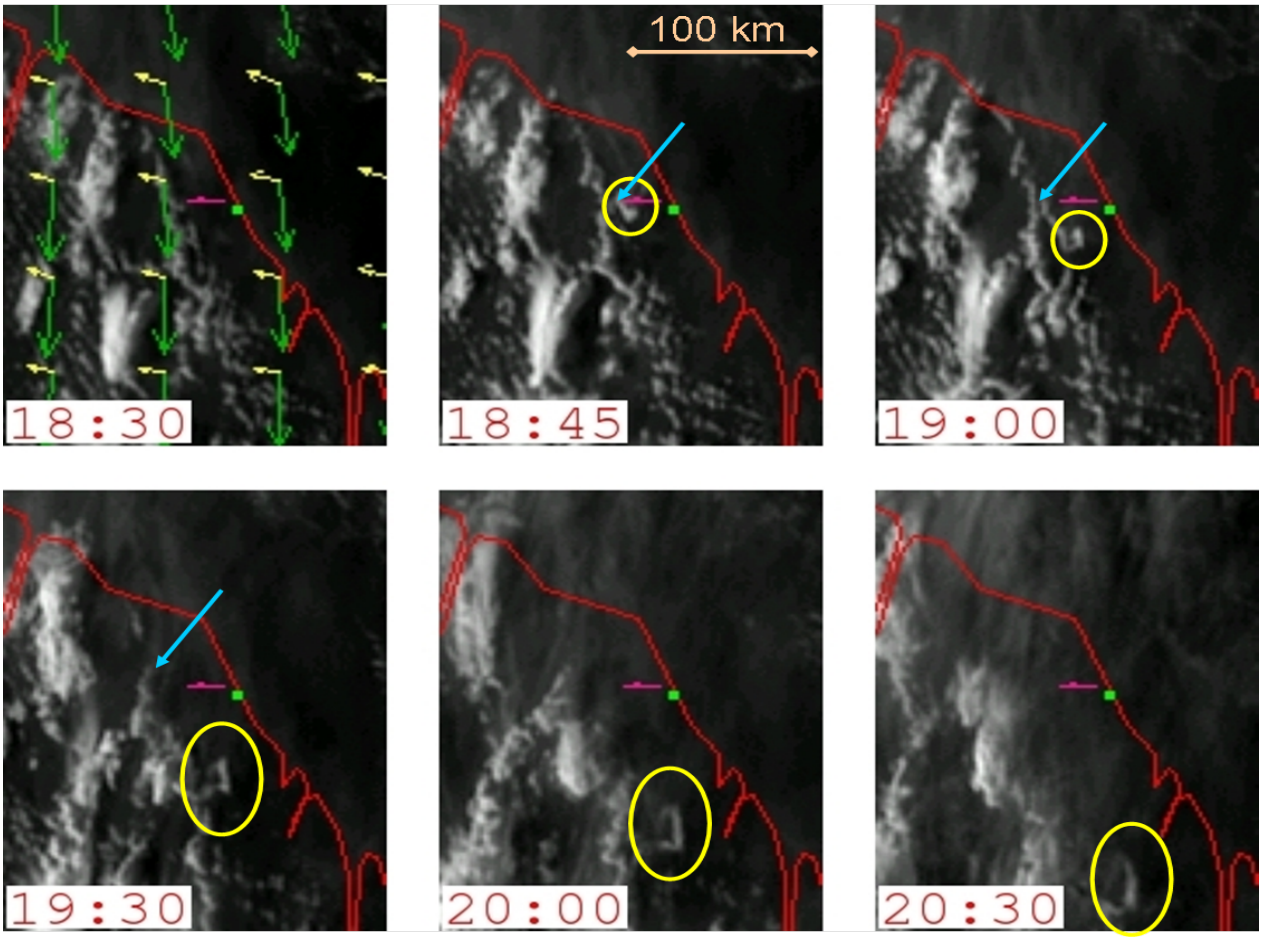

Figure 1: Satellite images from METEOSAT-9 SEVIRI instrument, HRV channel on 26 November 2010.
All scenes: Green dots indicate position of Kourou City in French Guyana.
The pink line represents trajectory of the Ariane5 launch vehicle from 0 to 20 km altitude.
Whereas Ariane5 originally started eastwards, trajectory is seen westwards due to parallax effects.
Scene at 18:30 UTC (before start):
Mainly natural cloudiness, wind direction in 850 hPa (yellow arrows), wind direction in 100 hPa (green arrows).
Scenes at 18:45 UTC and thereafter:
The yellow circles indicate position of the Ariane5 rocket contrail near 14 km altitude.
The blue arrows mark the position of the low-level rocket plume below 4 km altitude.

To obtain information on the altitudes of these two objects, we use reanalysis data from numerical weather prediction model operated by the European Centre for medium-range weather forecast ECMWF, which integrates information from different observational sources into the data assimilation. The ECMWF wind fields at low altitudes are directed towards the west, hence support the visual impression that the westward moving cloud structure (blue arrows) is caused by the particulate rocket exhaust plume in altitudes below 2 to 4 km.
In contrast, the line-shaped contrail structure drifts in southern direction. ECMWF reanalysis of wind fields shows winds from north only in a small altitude range represented by the 100 hPa pressure level. This corresponds to an altitude of 14 km hence above the level of local air traffic. In addition, we investigate the relative humidity fields in the upper troposphere and tropopause region on that day in order to evaluate the potential of ice cloud and contrail formation. The relative humidity data are again provided by ECMWF reanalysis. Figure 2 shows relative humidities with respect to water above 100% in a large area above French Guyana, which strongly supports the possibility of rocket contrail formation. Within the next 2 hours the rocket contrail can be identified in each satellite image. It drifts in southern directions till darkness prevents the detection of its further evolution.
Due to the local cloud structure and caused by restricted rocket launch rates, we estimate that the global impact of rocket contrails on atmospheric composition and climate is very small. Still, the combined evidence from the satellite images and ECMWF reanalysis data suggests that contrails can form on rocket exhaust plume particles and that rocket contrail formation can be detected in meteorological geostationary satellite data.

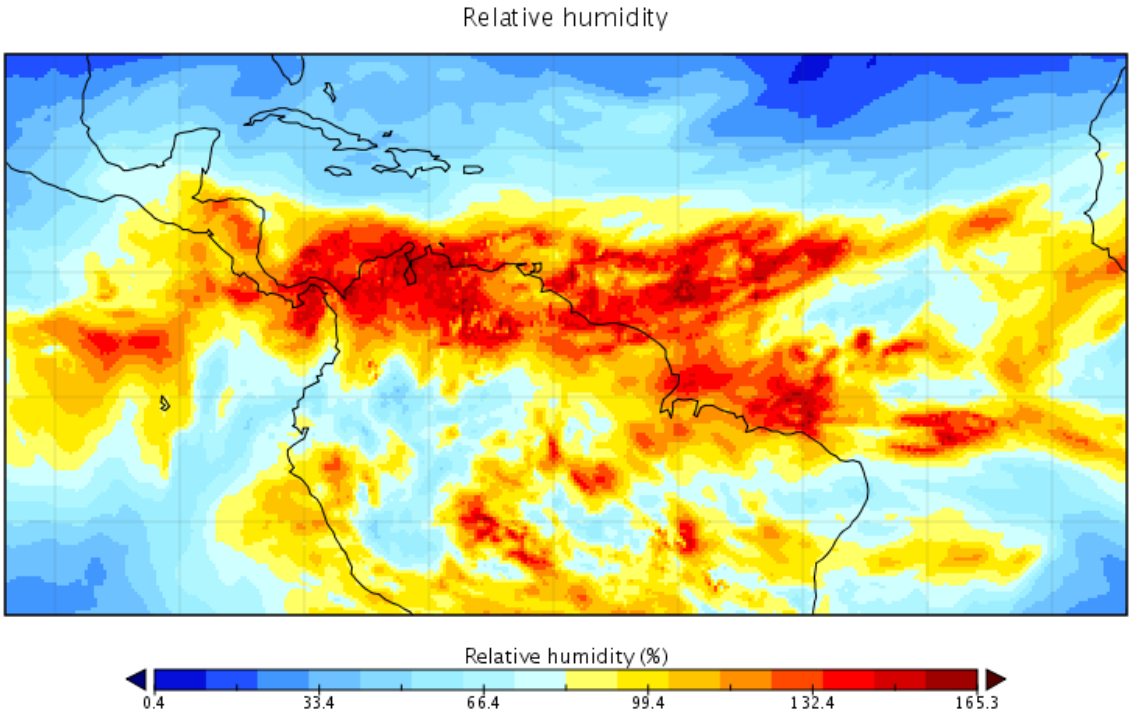

Figure 2: Relative humidity on 26 November 2010 at 18:00 UTC from ECMWF reanalysis at the 100 hPa level

5. Detection of polar mesospheric cloud formation related to rocket emissions

First evidence of ice cloud formation related to rocket emissions in the tropopause region has been shown in the previous section. Similar effects have been reported previously in the mesosphere at altitudes above 80 km, and enhanced water vapour and ice cloud occurrence has been related to the launch of space vehicles. Direct evidence of a mesospheric water vapour change caused by rocket emissions has been found in water vapor radiance data obtained from the Sounding of the Atmosphere with Broadband Emission Radiometry (SABER) instrument on the Thermosphere Ionosphere Mesosphere Energetics and Dynamics (TIMED) satellite [18]. Over a 10 month period in 2002 the radiometer detected radiance enhancements between 90 and 130 km altitude related in time and location to emissions from space shuttles or from liquid fuelled rocket launches. About 40% of the total liquid fueled launches, including four out of four space shuttle launches could be identified in the radiance data and lead to enhanced water vapor layers in the mesosphere.

Another evidence of the impact of rocket exhaust in the mesosphere is the observations of a water vapor plume with the Middle Atmosphere High Resolution Spectrograph Investigation (MAHRSI) instrument in the payload bay of the space shuttle Discovery (STS-85) [19]. An Arctic mesospheric OH plume has been observed one day after the space shuttle launch in 1997 at altitudes above 85 km. At these altitudes OH is produced predominantly by the photolysis of water vapor, hence can be used as indicator for water vapor. One week later a polar mesospheric cloud (PMC) has been observed between 70 and 75°N with the CRyogenic Infrared Spectrometers and Telescopes for the Atmosphere-Shuttle PAllet Satellite (CRISTA-SPAS) instrument in the Discovery payload. The inferred ice water content was of the same magnitude as water vapor injected by space shuttle (~10^{31} molecules or 3.5 ppmv at these altitudes). Trajectory calculations link the PMC observation site to the initial water vapor enhancement by the space shuttle exhaust. Hence the observations suggest that rocket exhaust plumes can significantly perturb the mesospheric water vapor and cloud budget.

Transport of a space shuttle exhaust plume to the southern hemisphere has been observed by the Global Ultraviolet Imager (GUVI) on the TIMED satellite [20]. The instrument detects mesospheric water vapor using scattered solar Lyman α radiation. Mesospheric water vapor emissions from the Columbia space shuttle (STS-107) launched from Kennedy Space Center in January 2003 were followed over 2 days, intially spreading and moving north-east and after one day

changing to southern directions reaching 35°S. Ground-based light detection and ranging (lidar) observations from Rothera, Antarctica, show iron (Fe) layers near 112 km altitude 3 to 4 days after the STS-107 launch with high Fe concentrations of $1.5*10^4$ cm^{-3}. As there is no known natural source of neutral Fe above 100 km, these observations have been interpreted as Fe ablated from the shuttle's main engines. The lidar also detected enhanced PMC occurrence in Antarctica after the space shuttle launch.

Lidar, Radar, and optical observations have also been performed in Alaska in the polar summer mesosphere shortly after a space shuttle launch in 2007 [21]. Such a single space shuttle launch deposits ~0.3 Gg of water vapor in altitudes between 100 and 110 km. An exceptionally intense mesospheric cloud has been detected 3 days after the launch of the space shuttle (SST-118) on 8 August. As observed before, the space shuttle launch has been followed by enhanced formation of polar mesospheric clouds and the build up of iron layers in polar regions. The observed Fe layer increased by a factor of 20 in density compared to background levels. In addition, the radar records detected polar mesospheric summer echoes (PMSE) in this event.

6. Summary and outlook

Strong local and regional perturbations of atmospheric trace gas and particle fields have been detected in recent years after the launch of rockets by in-situ instruments on aircraft and by remote sensing observations from satellite. Alumina particles and chlorine compounds from SRM emissions can cause complete ozone destruction in the young exhaust plume and potentially lead to a global total ozone loss < 1%. Still insufficient knowledge on ozone loss processes (heterogeneous Cl chemistry, alumina particle composition, particle reactivity, use of other propellants, extrapolation of processes from the plume to the global scale) renders the final conclusion on global ozone loss open. Hence in situ measurements of rocket exhaust plumes would help to establish and assess formalisms to evaluate the relative ozone depletion caused by different rocket propellant types.

While the present day ozone loss caused by rocket emissions may be small, future ozone changes may not be particularly when considering potential strong increases in the rocket launch rate e.g. by space tourism or by geo engineering measures such as solar panels in space. In addition, rocket induced ozone loss might become important in near future when the anthropogenic stratospheric halogen loading decreases.

Enhanced water vapor and iron levels have been observed after the launch of space shuttles and large rockets collocated or followed by enhanced mesospheric cloud formation both in polar and extra-polar regions of the mesosphere. In addition, we present the first direct evidence for ice formation in the upper troposphere caused by rocket emissions. The unique observation of an Ariane5 rocket contrail in 14 km altitude and the detection of a particulate rocket cloud at ground levels from Meteosat SEVIRI images has to be verified in other rocket launch scenarios in order to better quantify the local and global effects of rocket emissions on the atmosphere.

References

[1] Sanderson, K. 2010. Science lines up for seat to space. *Nature*. Special report. 463:716–717.

[2] Ross, M., D. Toohey, M. Peinemann, P. Ross. 2010. Limits on the Space Launch Market Related to Stratospheric Ozone Depletion. Astropolitics. 7:50–82.

[3] Ross, M. N., P. D. Whitefield, D. E. Hagen, and A. R. Hopkins. 1999. In situ measurement of the aerosol size distribution in stratospheric solid rocket motor exhaust plumes. *Geophys.Res.Lett.* 26:7–13 doi:10.1029/1999GL900085.

[4] Ross, M. N., et al. 1999. Observation of stratospheric ozone depletion associated with Delta II rocket emissions *Geophys. Res. Lett.* 27:15–19. doi:10.1029/1999GL011159.

[5] Schmid, O., J. M. Reeves, J. C. Wilson, C. Wiedinmyer, C. A. Brock, D. W. Toohey, L. M. Avallone, A. M. Gates, and M. N. Ross. 2003. Size-resolved particle emission indices in the stratospheric plume of an Athena II rocket. *J. Geophys. Res.* 108:4250–4256. doi:10.1029/2002JD002486.

[6] Cziczo, D. J., D. M. Murphy, D. S. Thomson, and M. N. Ross. 2002. Composition of individual particles in the wakes of an Athena II rocket and the space shuttle. *Geophys.Res.Lett.* 29:2047–2051. doi:10.1029/2002GL015991.

[7] Popp, P. J., et al. 2002. The emission and chemistry of reactive nitrogen species in the plume of an Athena II solid-fuel rocket motor. *Geophys. Res. Lett.* 29:1887–18891. doi:10.1029/2002GL015197

[8] Gates, A. M., et al. 2002. In situ measurements of carbon dioxide. 0.37–4.0 μm particles, and water vapor in the stratospheric plumes of small rockets. *J. Geophys. Res.* 107:4649–4656. doi:10.1029/2002JD002121.

[9] Voigt, C., J. Schreiner, A. Kohlmann, P. Zink, K. Mauersberger, N. Larsen, T. Deshler, C. Kröger, J. Rosen, A. Adriani, F. Cairo, G. Di Donfrancesco, M. Viterbini, J. Ovarlez, H. Ovarlez, C. David, A. Dörnbrack. 2002. Nitric Acid Trihydrate (NAT) in Polar Stratospheric Clouds. *Science*. 290:1756-1758.

[10] Prather, M., M.M. Garcia, A. R. Douglas, C.H. Jackman, M.K. W. Kp and N.D. Sze. 1990. The Space Shuttle's Impact on the Stratosphere. *J. Geophys. Res.* 95:18,583–18,590.

[11] Jackman, C., D. Considine, and E. Fleming. 1996. Space shuttle's impact on the stratosphere: An update. J. Geophys. Res. 101. D7. doi:10.1029/96JD00577.

[12] Jackman, C. H., D. B. Considine, and E. L. Fleming. 1998. A global modeling study of solid rocket aluminum oxide emission effects on stratospheric ozone, Geophys. Res. Lett., 25(6): 907–910.

[13] Ross, M. N., M. Y. Danilin, D. K. Weisenstein, and M. K. W. Ko. 2004. Ozone depletion caused by NO and H_2O emissions from hydrazine fueled rockets. J. Geophys. Res. 109. D21305. doi:10.1029/2003JD004370.

[14] Ross, M., M. Mills, and D. Toohey. (2010). Potential climate impact of black carbon emitted by rockets, *Geophys. Res. Lett.* 37. L24810. doi:10.1029/2010GL044548.

[15] Jäger, H. 2005. Long term record of lidar observations of the stratospheric aerosol layer at Garmisch Partenkirchen. *J. Geophys. Res.* 110. D08106. doi:10.1029/2004JD005506.

[16] Voigt., C., H. Schlager, B. Luo, A. Dörnbrack , A. Roiger, P. Stock, J. Curtius, H. Vössing, S. Borrmann, P. Konopka, C. Schiller, G. Shur, T. Peter, Nitric Acid Trihydrate (NAT) formation at low NAT supersaturation in Polar Stratospheric Clouds. 2005. *Atmos. Chem. Phys*. 5:11371–1380.

[17] Schumann, U. 1996. On conditions for contrail formation from aircraft exhaust. *Met. Zeit.* 5. 23:395–414.

[18] Siskind, D. E., M. H. Stevens, J. T. Emmert, D. P. Drob, A. J. Kochenash, J. M. Russell, L. L. Gordley, and M. G. Mlynczak. 2003. Signatures of shuttle and rocket exhaust plumes in TIMED/SABER radiance data. *Geophys. Res. Lett.* 30:1819–1823. doi:10.1029/2003GL017627.

[19] Stevens, M. H., J. Gumbel, C. R. Englert, K. U. Grossmann, M. Rapp, and P. Hartogh. 2003. Polar mesospheric clouds formed from space shuttle exhaust. *Geophys.Res.Lett.* 30:1546–1550. doi:10.1029/2003GL017249.

[20] Stevens, M. H., R. R. Meier, X. Chu, M. T. DeLand, and J. M. C. Plane. 2005. Antarctic mesospheric clouds formed from space shuttle exhaust. *Geophys. Res. Lett.* 32. L13810. doi:10.1029/2005GL023054.

[21] Kelley, M. C., M. J. Nicolls, R. H. Varney, R. L. Collins, R. Doe, J. M. C. Plane, J. Thayer, M. Taylor, B. Thurairajah, and K. Mizutani. 2010. Radar, lidar, and optical observations in the polar summer mesosphere shortly after a space shuttle Launch. *J. Geophys. Res.* 115. A05304. doi:10.1029/2009JA014938.